

# Prediction of Electric Field in the Loaded Cavity Based on the Theory of Reverberation Chambers

Yan Chen<sup>1</sup>, Xiang Zhou<sup>2, \*</sup>, Jingkang Ji<sup>2</sup>, Shouyang Zhai<sup>1</sup>, and Dan Chen<sup>1</sup>

**Abstract**—The shielding cavity loaded with electronic equipment inside has a high  $Q$  value and is in overmode at relatively high frequency as a reverberation chamber (RC), but it does not have stirrers or paddles. However, the electromagnetic environment in the cavity is similar to that in the reverberation chamber working in frequency stirring mode or source stirring mode because of the certain bandwidth of the electronic equipment and the movement of the portable electronic equipment. Therefore, the electric field in the cavity can be predicted based on the theory of reverberation chamber. In order to predict the electric field in a given shielding cavity after loading additional electronic equipment, the determination method of the  $Q$  value of the cavity and the absorption cross section (ACS) of the electronic equipment, the influence of the ACS on the  $Q$  value of the cavity, and the relationship between the  $Q$  value and electric field are analyzed. Firstly, the ACS and radiated emission power of the loading electronic equipment are measured in the RC. Then, the  $Q$  value of the cavity with the electronic equipment loaded inside is calculated by the known  $Q$  value of the cavity without the electronic equipment and the ACS of the electronic equipment. Finally, the electric field in the cavity loaded with electronic equipment is estimated by using the calculated  $Q$  value of the loaded cavity and the measured radiated emission power of the electronic equipment. The experimental results verify the effectiveness of the prediction method.

## 1. INTRODUCTION

With the development of electronic technology, it is often necessary to bring a mobile phone or other electronic equipment into the electronic equipment cabin. Due to the resonance effect, a large maximum electric field would be formed in the cavity even if the radiation power of the electronic equipment is very small. This may cause interference with the electronic equipment in the cabin. If the influence of additional electronic equipment on the electromagnetic environment in the cabin can be predicted, the occurrence of interference can be avoided. This paper discusses a method of predicting the electric field that will be formed in the cabin when additional electronic equipment is introduced.

Generally, the shielded cabin can be regarded as a cavity with high  $Q$  value. At a given frequency, the electromagnetic distribution in a cavity is determined and can be calculated by the Maxwell's function. Well performed cavity works as a microwave resonator and is widely used in ships and spacecraft [1]. Usually, these cavities are equipped with many pieces of wireless electronic equipment like Bluetooth devices or communication equipment. However, due to the complex shape of the cavity, the indeterminacy of the radiation source bandwidth and the fact that the radiation sources always move with people or equipment, it is almost impossible and infeasible to obtain the determined field distribution in the cavity. To deal with the field distribution of this kind of cavity, reverberation

---

*Received 9 September 2020, Accepted 31 December 2020, Scheduled 14 January 2021*

\* Corresponding author: Xiang Zhou (zhouxiang@seu.edu.cn).

<sup>1</sup> State Key Laboratory of Nuclear Power Safety Monitoring Technology and Equipment, Shenzhen 518172, China. <sup>2</sup> School of Mechanical Engineer, Southeast University, Nanjing 211189, China.

chamber (RC) theory based on statistical electromagnetics is used to describe the electromagnetic environment [2].

The electromagnetic environment in the cavity with radiation sources, such as ship cabin or aircraft, has been assessed, and the results show that the maximum electric field is related with the performance of reverberant space [3]. It has been proved that complex geometry cavities without mechanical mode-stirrer could satisfy the statistical requirements of a well performed RC [4]. The normalized electric level in metallic cavities could be estimated by accurately evaluating the  $Q$  value of cavity ( $Q$ ) [5]. Meanwhile, the ACS of the lossy material can be calculated based on the  $Q$  value of the cavity with and without the lossy material inside [6]. The ACS measurements can be averaged with respect to different configurations, hence the relevant uncertainty depends on the number of dependent samples [7]. With proper stirring bandwidth, field in the cavity behaves as expected in the RC [8].

For the convenience of description, when a new piece of electronic equipment is introduced into a working cavity, the newly introduced electronic equipment is called loading object. The radiation emission of the loading material will affect the electromagnetic environment in the cavity and may cause interference to other electronic equipment in the cavity. This should be evaluated before the loading object is introduced into the cavity. For example, to change the wired communication in the shielding factory built into the wireless communication, it is necessary to add wireless relays in the shielding building, and the staff will carry communication terminals with them. This kind of shielding building is like a cabin. Staff, wireless relays, and communication terminals will load the shielding building, and wireless relays and communication terminals have radiation emission, which will affect the field distribution of the building. Before change, the electric field in the shielding building with the wireless communication should be predicted to estimate whether the new electric field will interfere with the original electronic equipment in the building.

This paper gives a method of predicting the electric field in the cavity loaded electronic equipment. First of all, the ACS of the loading object like electronic equipment could be obtained from the  $Q$  values of the RC before and after being loaded. Then, the  $Q$  value of the loaded cavity could be estimated by the ACS and the unloaded cavity  $Q$  value. Finally, the maximum and average electric fields in the cavity can be predicted from the estimated  $Q$  value of the loaded cavity and the radiation emission power of the loading object. It should be mentioned that the method in this paper is only suitable for the cavity working in overmodeed state. Detailed derivation is provided in the next section. The experimental method is introduced in Section 3, and the experimental results from 0.5 GHz to 1 GHz are given in Section 4. The reverberant characteristics of the RC used as a cavity in experiment have been validated in previous research [9].

## 2. THEORETICAL MODEL DESCRIPTION

### 2.1. Determinate the $Q$ Value of RC or Cavity

In the process of predicting the electric field in the loaded cavity, it is necessary to measure the  $Q$  value of RC and the cavity. As mentioned before, the electric field inside a cavity is a desired reverberant field or at the overmode state. Thus, we could use the theory proposed by Hill and get the frequency-domain  $Q$  [10, 11] by using two antennas and a vector network analyzer (VNA).

$$Q = \frac{16\pi^2 V \langle P_r \rangle}{\lambda^3 P_t} \quad (1)$$

$$Q = -\frac{16\pi^2 V |\langle S_{21} \rangle|^2}{\lambda^3 (1 - |\langle S_{11} \rangle|^2)(1 - |\langle S_{22} \rangle|^2) \eta_1 \eta_2} \quad (2)$$

Equation (1) is derived from the definition of the  $Q$  value and the steady-state cavity in which the injected energy and dissipated energy are equal. Here,  $V$  represents the volume of the cavity.  $P_r$  is the energy received from the antenna, and  $\lambda$  represents the wave length of testing frequency.  $\langle \cdot \rangle$  represents the character averaged at different frequency points. Considering the reflection coefficient and the efficiency of the testing antennas, we could get Equation (2). The scattering parameters  $S_{11}$ ,  $S_{21}$ ,  $S_{22}$  could be obtained from VNA and are averaged from several frequency points. It has to be known that the single  $S_{11}$  or  $S_{22}$  should be measured in the free space and is nearly equal to the average

parameters in RC or cavity [12]. Subsequently,  $\eta_1$  and  $\eta_2$  are the efficiencies of the transmitting and receiving antennas.

## 2.2. Calculate ACS Based on the $Q$ Value of RC

The  $Q$  value of RC is represented by  $Q_{empty}$  before the loading object is placed, and  $Q_{RC}$  represents that after the loading object is placed. Both  $Q_{empty}$  and  $Q_{RC}$  can be obtained by Equation (2). At the same time,  $Q_{RC}$  can be expressed by the following formula.

$$\frac{1}{Q_{RC}} = \frac{1}{Q_{object}} + \frac{1}{Q_{empty}} \quad (3)$$

Also it has been proved that  $Q_{object}$  could be described by the ACS  $\langle\sigma_a\rangle$  for the energy absorbed by the loading object [13]:

$$Q_{object} = \frac{2\pi V}{\lambda\langle\sigma_a\rangle} \quad (4)$$

where  $V$  and  $\lambda$  are the same as in Equation (1). Thus, the ACS of the loading object could be obtained by using Equations (3) and (4):

$$\langle\sigma_a\rangle = \frac{2\pi V}{\lambda} \left( \frac{1}{Q_{load}} - \frac{1}{Q_{unload}} \right) \quad (5)$$

Here the ACS,  $\langle\sigma_a\rangle$ , is averaged over the incident angle of  $4\pi$  spherical degree and all polarization. Meanwhile, it does not depend on the electromagnetic environment produced by RC. Finally, Equation (6) could be deduced from Equations (2) and (5):

$$\langle\sigma_a\rangle = \frac{\lambda^2}{8\pi} \eta_1 \eta_2 \left( \frac{1}{G_{load}} - \frac{1}{G_{unload}} \right) \quad (6)$$

Here  $G$  represents the gain of an RC:

$$G = \frac{|\langle S_{21} \rangle|^2}{(1 - |\langle S_{11} \rangle|^2)(1 - |\langle S_{22} \rangle|^2)} \quad (7)$$

Therefore, RC can be used to test the ACS of the loading object.

## 2.3. Estimate the $Q$ Value of the Cavity When the Objects with Known ACS are Placed

Using Equation (3), Equations (4) and the result obtained by Equation (6), it is possible to estimate the  $Q$  value of any cavity,  $Q_{load-cavity}$ , in which the loading object with known ACS is placed. The loaded cavity  $Q_{load-cavity}$  is shown below:

$$Q_{load-cavity} = \frac{1}{(1/Q_{cavity} + \lambda\langle\sigma_a\rangle_{object}/2\pi V)} \quad (8)$$

where  $Q_{cavity}$  is the  $Q$  value of the cavity without loading object;  $\langle\sigma_a\rangle_{object}$  is the ACS of the loading object;  $V$  and  $\lambda$  are the same as in Equation (1).

## 2.4. Predict the Electric Field in the Cavity

Because the electromagnetic environment in the cavity could be described as a kind of reverberant field, the electric field distribution including averaged electric field and maximum electric field can be deduced from the plane wave integral theory. It should be emphasized that the maximum electrical field is arisen from the extreme value distribution [14]. The averaged electric field,  $\langle E_{ave} \rangle$ , and the maximum electric field,  $\langle E_{max} \rangle$ , can be obtained by the following formulas.

$$\langle E_{ave} \rangle \approx \sqrt{\frac{\lambda \eta_V \eta_1 Q \langle P_t \rangle}{6\pi V}} \quad (9)$$

$$\langle E_{max} \rangle \approx \sqrt{\frac{\lambda \eta_V \eta_1 Q \langle P_t \rangle}{6\pi V} \left[ 0.577 + \ln(N+1) - \frac{1}{2(N+1)} \right]} \quad (10)$$

where  $\eta_V$  represents free space wave impedance,  $\eta_1$  the efficiency of transmitting antenna,  $N$  the number of the independent samples, and  $\langle P_t \rangle$  the power injected into the cavity. For the loaded cavity,  $\langle P_t \rangle$  is the average radiated power of the loading object, such as electric equipment. As shown in Equations (9) and (10), the electric field is associated with  $Q_{load-cavity}$  and the radiated power of the loading object for the loaded cavity.

Since the field in the cavity is a statistical field, the confidence interval of the estimated field should be considered. The upper and lower quantiles under 95 percent confidence intervals are described as Equations (11) and (12) by using the extreme value distribution under reverberant field.

$$\xi_{0.025}(E_{\max}) \approx \sqrt{-\frac{\lambda\eta_V\eta_1Q\langle P_t \rangle}{6\pi V}\ln(1 - 0.025^{1/N})} \quad (11)$$

$$\xi_{0.975}(E_{\max}) \approx \sqrt{-\frac{\lambda\eta_V\eta_1Q\langle P_t \rangle}{6\pi V}\ln(1 - 0.975^{1/N})} \quad (12)$$

The formulas above are appropriate for the situation that the electric field is away from the wall. The field at a distance less than  $\lambda/4$  from the wall is obviously inferior to that in the uniformly region because of the edge effect. Hence the maximum electric field in the cavity can be seen as the result in Equation (10). However,  $\lambda/4$  of the frequency higher than 0.5 GHz is smaller than 0.15 meters, and the space near the wall only occupies a small part of the whole cavity space.

### 3. MEASUREMENT APPROACH

Two RCs are employed for verifying the conclusion in Section 2 along with two pairs of log-periodic antennas. The bigger RC is the Comtest Engineering LUF 200 sized 6.16 m  $\times$  4.05 m  $\times$  3.15 m with an oscillating wall stirrer. It has been validated from 200 MHz to 18 GHz and proved to be in completely overmode state above 500 MHz [9]. This RC is used for getting the ACS of the loading object, and it is called RC1. The smaller RC is made of aluminum with a size of 1.5 m  $\times$  1.38 m  $\times$  2.32 m and has been validated from 500 MHz, which is used as a cavity to be loaded, and it is called CAVITY. VNA (Agilent E5071C) is connected to two antennas in the RC by cables, and the dual port calibration is carried out before the experiment.

Three groups of experiments have been carried out. The first group of experiments is to test the  $Q$  values of the RC1 loaded and unloaded to obtain the ACS of the loading object. The second group of experiments is carried out in CAVITY to verify the correctness of Equation (8), and the third group of experiments is to verify the correctness of the predicted electric field.

For clarity and convenience, the absorbing material is used to simulate the loading object. The test layout for the first group of experiments is shown in Fig. 1. The working frequency range of the log-periodic antennas is from 200 MHz to 1000 MHz. As shown in Fig. 1, the transmitting antenna is put towards the stirrer or the corner while the receiving antenna is placed inside the area with any direction. The absorbing material is placed on a table 9 meters high, and two antennas are 1.2 meters high.  $S_{11}$ ,  $S_{21}$ , and  $S_{22}$  of VNA are recorded at 2550 frequency points uniformly spaced from 495 MHz to 1005 MHz for CAVITY with and without the absorbing material. The antenna efficiencies  $\eta_1$  and  $\eta_2$  are 75 percent as recommended in [15]. The scattering parameters are averaged over the frequency band of more than 10 MHz, which is also more than a  $Q$  bandwidth. To ensure the accuracy of the test results, there is no change in the test process except for the absorbing material.

The test layout for the second group of experiments is shown in Fig. 2. The same absorbing material as the first group of experiments is placed on the floor of CAVITY. The previous research showed that the position of the absorbing material has little effect on the  $Q$  value. The working frequency range of the log-periodic antennas is from 400 MHz to 2000 MHz. The antennas are used to test the  $S$  parameters of CAVITY with and without absorbing materials to verify the correctness of Equation (8).

In Fig. 3, only one antenna is used. Because the absorbing material is passive, the antenna is used to simulate the radiation emission of the loading object of CAVITY, that is,  $\langle P_t \rangle$  in Equations (10) and (11). In practical application, the average radiation emission power  $\langle P_t \rangle$  of the electronic equipment can be tested by RC according to IEC 61000-4-21. The electric field probe, Narda ep-603, is used to test the field in CAVITY to verify the correctness of Equation (10). Except that the receiving antenna is replaced by a probe, the configurations in Fig. 2 and Fig. 3 are the same. The probe is set 0.4 meter



**Figure 1.** Measurement of the  $Q$  values of unloaded and loaded RC1.



**Figure 2.** Measurement of the  $Q$  values of unloaded and loaded CAVITY.

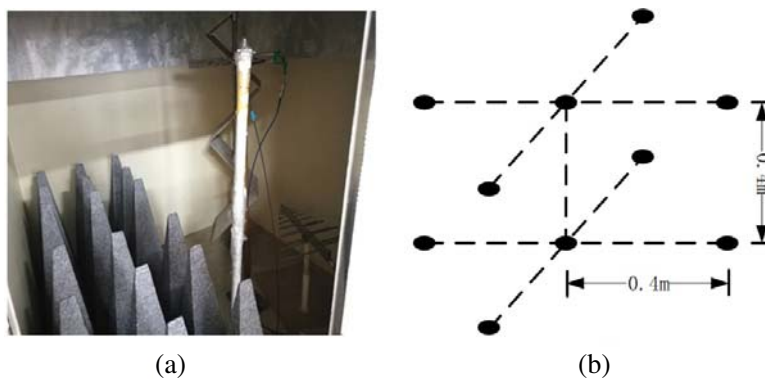


**Figure 3.** (a) Measurement of electric field of the loaded CAVITY, (b) layout of electric field measurement points.

away from each other and far away from the metal wall. The net input power of transmitting antenna and the reading of the probe are recorded at given frequency. The interval of frequency is set at 200 kHz with 20 samples which is also the same as the  $Q$  value measurement.

#### 4. RESULTS

Based on the measurement results of  $S$  parameters under loading and unloading states,  $Q$  values of loaded and unloaded RC1 can be obtained from Equation (2), which are shown in Fig. 4. It is conspicuous that the loaded RC1 has much lower  $Q$  than the unloaded RC1 for the absorption loss. Meanwhile, two curves keep good consistency which demonstrates that the loading objects do not change the field distribute obviously. After getting two essential  $Q$  values, the ACS of the absorbing material is accessible automatically by applying Equation (6). The results can be seen in Fig. 5. The dotted line is ACS calculated and mainly distributes around one square meter. The curve achieved by using the frequency domain method introduces more burrs inevitably because of resonance. The red heavy line is the polynomial fitting value which will be used to figure out the  $Q$  value of the loaded CAVITY.

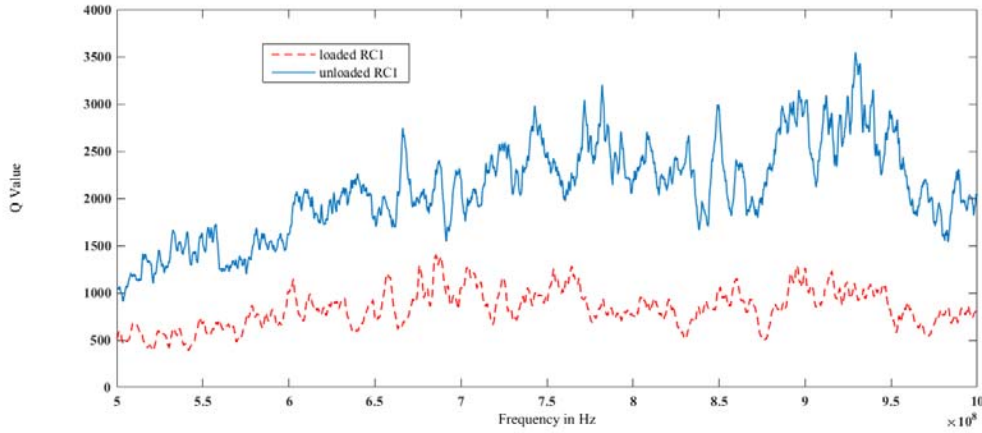


**Figure 4.**  $Q$  values of the loaded and unloaded RC1.

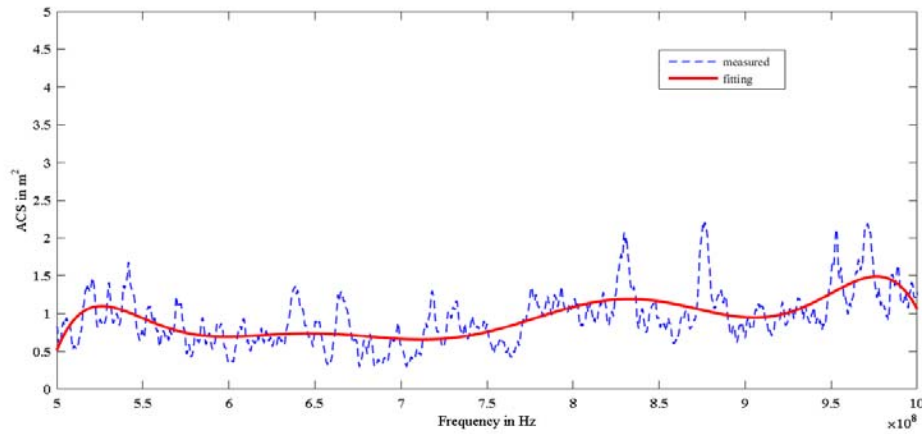


**Figure 5.** Measured ACS and the polynomial fitting one.

The  $Q$  value of the loaded CAVITY can be measured by the same method as RC1 or estimated by ACS of the loading object and the  $Q$  value of unloaded CAVITY. In Fig. 6, the measured  $Q$  value of the unloaded CAVITY is expressed by the brown dash-dotted line. The calculated  $Q$  value of the

loaded CAVITY is expressed by the red solid line, and the blue dashed line is the measured  $Q$  value of the loaded CAVITY. The calculated  $Q$  value is mainly distributed between 20 and 200 while the measured item is mainly distributed between 10 and 300. In general, the two  $Q$  values are consistent, which indicates the credibility of the estimation of the  $Q$  value.

As mentioned earlier, the average and maximum electric fields in loaded CAVITY can be predicted from Equations (9) and (10) based on the calculated ACS of loading object and the  $Q$  values of the CAVITY without loading object. In order to verify the predicted results, the average electric field and maximum electric field are measured by the electric field probe at the same time.

The predicted and the measured average electric fields are shown in Fig. 7. The biggest gap between the two curves happens at 1 GHz with about 7 V/m. The predicted average electric field is in good agreement with the measured value. Since electronic devices are sensitive to the maximum electric field, special attention is paid to the maximum electric field. The predicted maximum electric field, measured maximum electric field, and 95 percent confidence intervals are shown in Fig. 8. The predicted maximum electric field agrees with the measured one except at 500 MHz. At this frequency point, the loading object may make the CAVITY no longer meet the reverberant condition. Simultaneously, measured electric field at all the other frequency points is between the upper and lower quantiles at 95 percent confidence intervals. Therefore, both the average electric field and the maximum electric field prediction results are credible, which proves the correctness of the prediction method.

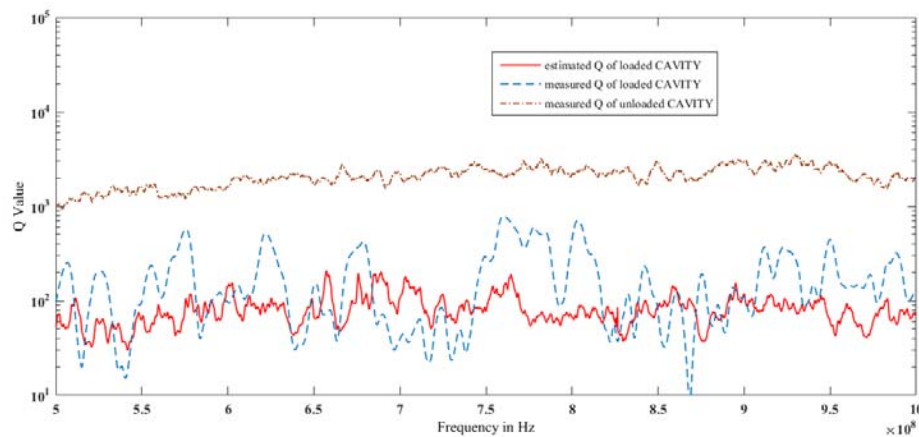


**Figure 6.** Comparison of the measured and estimated  $Q$  value of CAVITY.

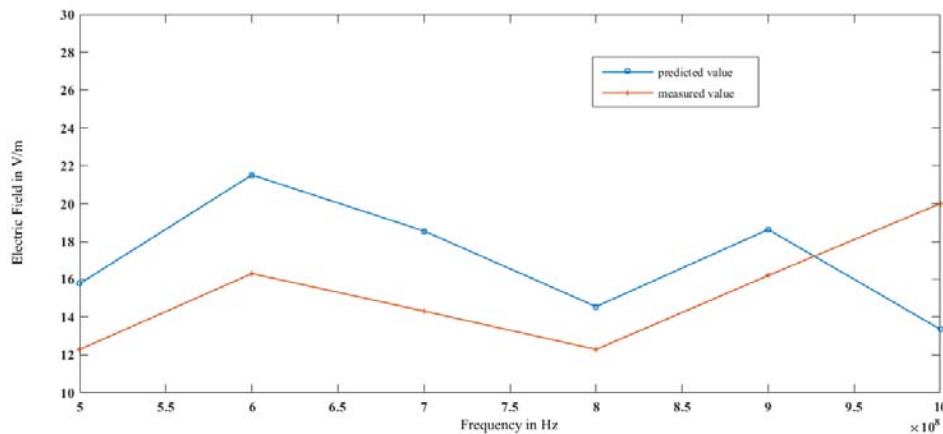


**Figure 7.** Comparison of the measured and predicted averaged electric field.



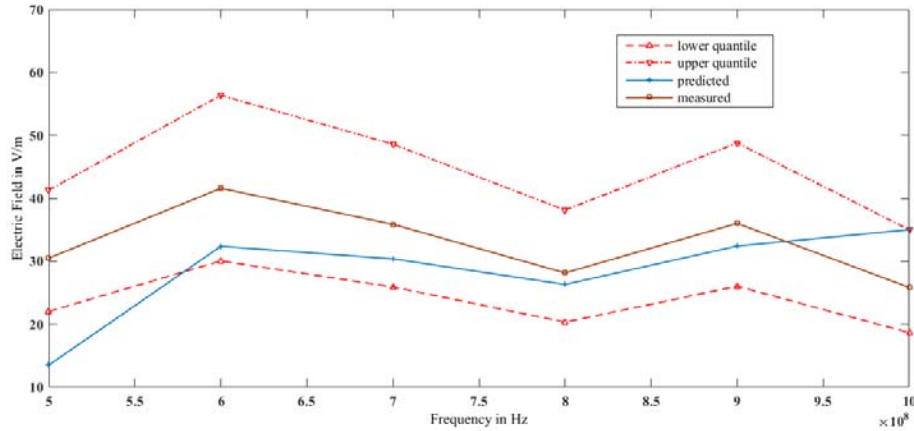


**Figure 8.** Comparison of the measured and predicted maximum electric field with the upper and lower quantiles at 95 percent confidence intervals.

## 5. CONCLUSION

In this paper, a method of predicting the electric field of loaded cavity based on the theory of RC is proposed. It is difficult to measure the electric field in the cavity with various shapes and radiation sources especially under the actual working conditions. The electromagnetic field in the shielded cavity at relatively high frequency can form a kind of reverberant field, and we can deal with it by the reverberation chamber theory. The concrete steps are as follows: 1) Determine the state of electromagnetic reverberation in the cavity at given bandwidth. 2) Calculate the ACS of loading object based on the measured  $Q$  values in RC. 3) Calculate the  $Q$  value of the loaded cavity by the acquired ACS of loading object and the  $Q$  value of the unloaded cavity. 4) Predict the generated electrical field by the known or measured radiation emission power of the loading object.

Three groups of experiments have been carried out to prove the effectiveness of the method. The first group is to get the ACS of the loading object. The second group is to estimate the  $Q$  value of the loaded cavity and to verify the correctness of the estimated value, and the third one is to predict the average and maximum electric fields in the correctness and to prove the creditability of the predicted value. Results show that the predicted averaged electric field agrees with actual measured electric field, and the maximum electrical field predicted is between the upper and lower quantiles with 95 percent confidence intervals except at the initial frequency. The reason may be that the loading object changes the field distribution of the cavity at that frequency. Therefore, the prediction method is feasible and effective.

## ACKNOWLEDGMENT

This research is supported by the National Natural Science Foundation of China (No. 51677029).

## REFERENCES

1. Siah, E. S., K. Sertel, J. L. Volakis, V. V. Liepa, and R. Wiese, "Coupling studies and shielding techniques for electromagnetic penetration through apertures on complex cavities and vehicular platforms," *IEEE Transactions on Electromagnetic Compatibility*, Vol. 45, No. 2, 245–256, 2003.
2. Hill, D. A., *Electromagnetic Fields in Cavities: Deterministic and Statistical Theories*, Wiley-IEEE Press, New Jersey, 2009.
3. Tait, G. B., C. E. Hager Iv, T. T. Baseler, and M. B. Slocum, "Ambient power density and electric field from broadband wireless emissions in a reverberant space," *IEEE Transactions on Electromagnetic Compatibility*, Vol. 58, No. 1, 307–313, 2016.



4. Gros, J. B., O. Legrand, F. Mortessagne, E. Richalot, and K. Selemani, "Universal behaviour of a wave chaos based electromagnetic reverberation chamber," *Wave Motion*, Vol. 51, No. 4, 664–672, 2014.
5. Romero, S. F., G. Gutierrez, and I. Gonzalez, "Universal behaviour of a wave chaos based electromagnetic reverberation chamber," *Prediction of the Maximum Electric Field Level Inside a Metallic Cavity Using a Quality Factor Estimation*, Vol. 28, No. 12, 1468–1477, 2014.
6. Gradoni, G., D. Micheli, F. Moglie, and V. Mariani Primiani, "Absorbing cross section in reverberation chamber: Experimental and numerical results," *Progress In Electromagnetics Research B*, Vol. 45, 187–202, 2012.
7. Gifuni, A., H. Khenouchi, and G. Schirinzi, "Performance of the reflectivity measurement in a reverberation chamber," *Progress In Electromagnetics Research*, Vol. 154, 87–100, 2015.
8. Yu, S. P. and C. F. Bunting, "Statistical investigation of frequency-stirred reverberation chambers," *2003 IEEE Symposium on Electromagnetic Compatibility. Symposium Record (Cat. No. 03CH37446)*, Vol. 1, 155–159, 2003.
9. Zhou, Z., P. Hu, X. Zhou, J. Ji, and Q. Zhou, "Performance evaluation of oscillating wall stirrer in reverberation chamber using correlation matrix method and modes within Q-bandwidth," *IEEE Transactions on Electromagnetic Compatibility*, Vol. 62, No. 6, 2669–2678, 2020, doi: 10.1109/TEM.2020.2983981.
10. West, J. C., J. N. Dixon, N. Nourshamsi, D. K. Das, and C. F. Bunting, "Best practices in measuring the quality factor of a reverberation chamber," *IEEE Transactions on Electromagnetic Compatibility*, Vol. 60, No. 3, 564–571, 2018.
11. Ji, J., X. Zhou, and P. Hu, "Frequency-dependent oscillating wall stirrer for measurement of quality factor in a reverberation chamber," *2019 IEEE International Conference on Computation, Communication and Engineering (ICCE)*, 142–145, 2019.
12. West, J. C., V. Rajamani, and C. F. Bunting, "Frequency- and time-domain measurement of reverberation chamber Q: An in-silico analysis," *2016 IEEE International Symposium on Electromagnetic Compatibility*, 7–12, 2016.
13. Hill, D. A., M. T. Ma, A. R. Ondrejka, B. F. Riddle, M. L. Crawford, and R. T. Johnk, "Aperture excitation of electrically large, lossy cavities," *IEEE Transactions on Electromagnetic Compatibility*, Vol. 36, No. 3, 169–178, 1994.
14. Arnaut, L. R., "Measurement uncertainty in reverberation chambers," Report TEQ 2, Ed, 2.0, National Physical Laboratory (UK), 2008.
15. IEC 61000-4-21, "Electromagnetic compatibility (EMC) — Part 4-21: Testing and measurement techniques — Reverberation chamber test methods," International Electromagnetic Commission (IEC), 2011.